nature

https://doi.org/10.1038/s41586-024-07628-1

Accelerated Article Preview

Unlocking carbene reactivity by metallaphotoredox α-elimination

Received: 23 February 2024

Accepted: 30 May 2024

Accelerated Article Preview

Cite this article as: Boyle, B. T. et al. Unlocking carbene reactivity by metallaphotoredox α-elimination. *Nature* https://doi.org/10.1038/s41586-024-07628-1 (2024)

Benjamin T. Boyle, Nathan W. Dow, Christopher B. Kelly, Marian C. Bryan & David W. C. MacMillan

Unlocking carbene reactivity by metallaphotoredox α-elimination

Benjamin T. Boyle[*1], Nathan W. Dow[*1], Christopher B. Kelly[2], Marian C. Bryan[3], and David W. C. MacMillan[†,1]

Affiliations:

[1]Merck Center for Catalysis at Princeton University, Princeton, New Jersey 08544, United States

[2]Discovery Process Research, Janssen Research & Development LLC, Spring House, Pennsylvania 19477, United States

[3]Therapeutics Discovery, Janssen Research & Development LLC, Spring House, PA 19477, United States

[*]These authors contributed equally to this work.

[†]Corresponding author: dmacmill@princeton.edu

The ability to tame high-energy intermediates is critical for synthetic chemistry, enabling the construction of complex molecules and propelling advances in the field of synthesis. Along these lines, carbenes and carbenoid intermediates are particularly attractive, but often elusive, high-energy intermediates.[1,2] Classical methods to access metal carbene intermediates exploit two-electron chemistry to form the critical carbon–metal bond. However, these methods are often prohibitive due to reagent safety concerns, limiting their broad implementation in synthesis.[3–6] Mechanistically, an alternative approach to carbene intermediates that could circumvent these pitfalls would involve two single-electron steps: radical addition to a metal to forge the initial carbon–metal bond followed by redox-promoted α-elimination to yield the desired metal carbene intermediate. Herein, this strategy is realized through a metallaphotoredox platform that exploits iron carbene reactivity using readily available chemical feedstocks as radical sources and α-elimination from six classes of previously underexploited leaving groups. These discoveries permit cyclopropanation and σ-bond insertion into N–H, S–H, and P–H bonds from abundant and bench-stable carboxylic acids, amino acids, and alcohols, thereby providing a general solution to the challenge of carbene-mediated chemical diversification.

Controlled access to high-energy chemical intermediates, such as carbanions, carbocations, radicals, and carbenes, is a key step in many critical bond forming processes.[7–10] Accessing these intermediates requires reactive starting materials that possess high-energy ground states, which limits functional group compatibility, particularly in the context of complex synthetic targets. Modern advances in organic chemistry have allowed controlled access to some synthetically useful high-energy species, most notably, radical intermediates.[11–14] Photoredox catalysis harnesses the energy of visible light for reactivity up-conversion, turning inert and stable starting materials into reactive radical species. The extension to metallaphotoredox catalysis, which merges transition metal cross-coupling with these radical intermediates, provides entry to an immense depth of previously inaccessible chemical space.[8] By contrast, broad access to carbenes and carbenoids remains elusive, despite their similar transformative potential in a wide range of bond formations.[2,15] Traditional methods for accessing carbene intermediates rely on high-energy, bifunctional or pseudo-bifunctional precursors, such as diazo (or pro-diazo) compounds, polyhalogenated precursors, or sulfonium ylides.[3,5,16] Ultimately, the reactivity and structural specificity of these starting materials limits utility and, in some cases, raises safety concerns, such as the need for high temperatures and/or explosive reagents. Although Motherwell, and more recently, Nagib have demonstrated that carbonyl intermediates can serve as carbene precursors through pre-generated zinc carbenoids,[17–21] there remains no general strategy to access carbene intermediates from other naturally occurring and abundant starting materials, such as carboxylic acids, amino acids, and alcohols. To address longstanding limitations in carbene

chemistry, we envisioned separating the process of carbene generation into two sequential single-electron operations, exploiting the potential of visible-light photocatalysts to control radical formation and manipulate the oxidation state of metal catalysts. Herein, we report a general visible light-mediated strategy to access iron carbenes from abundant precursors via sequences of radical addition and reduction-induced α-elimination operating across six distinct types of non-traditional leaving groups. This approach allows cyclopropanation and X–H insertion reactions under mild conditions with broad functional group tolerance. More generally, this approach introduces the carbene equivalent of radical metallaphotoredox chemistry and circumvents many of the drawbacks of traditional strategies for carbene formation.

To develop a single-electron approach to carbene formation, we first examined existing strategies in an effort to identify the critical design aspects. The most common methods to access carbene intermediates involve starting materials with ylide-type character, such as diazo-type compounds with a negative charge next to a diazonium ion.[22,23] The bifunctional nature of these species allows for rapid formation of a metal carbene complex via nucleophilic attack on the metal center followed by heterolytic α-elimination (which is contingent on the appropriate metal oxidation state) to forge the second metal–carbon bond. The requirement for ylide-type reactivity limits the pool of potential starting materials for carbene reactivity, and the general functional group tolerance of any method developed with this chemistry. We questioned whether it would be possible to mimic ylide-type reactivity by using single-electron intermediates bearing a leaving group at the incipient radical center. To generate a carbenoid equivalent, radical metalation would yield the first metal–carbon bond, precluding the requirement for nucleophilic reactivity.[8] Because of the low energy barrier for radical metalation, the event would occur at or close to the rate of diffusion, limiting off-cycle radical coupling or addition-type processes.[24,25] Single-electron reduction of the metal center would then trigger α-elimination, ejecting the leaving group and furnishing the desired metal carbene species. The timing of radical generation and manipulation of the redox state of the metal is critical to success here and, as such, photocatalysis was pursued as a means to orchestrate these events (Fig. 1a).[8] Although radical addition to metal centers is well-established in photocatalytic regimes,[8] there are few reports of single-electron reduction-induced α-elimination, resulting in poor understanding of the leaving groups and by extension, carbene precursors, that would be tolerated within this step.[26–29] Realization of this envisioned reaction archetype would permit access to a wealth of modes of radical generation, dramatically expanding the limited palette of metal carbenes and, in turn, the types of transformations enabled by these organometallic complexes. As such, achieving the desired carbene reactivity from radical precursors necessitated investigation into the proposed redox-induced α-elimination.

Probing radical approach to carbene intermediates

To realize this new carbene paradigm, three components would need to be addressed: (1) radical generation from the appropriate precursor, (2) identification of an appropriate metal for radical binding and redox window for controlled oxidation state changes, and (3) establishment of the ability of that metal to engage in α-elimination with synthetically convenient leaving groups upon oxidation state change. To evaluate the viability of our proposed sequence, α-acetoxy carboxylic acids were chosen due to the ease of radical formation from carboxylic acids, a benefit amplified by the nucleofugality of the acetate group and the synthetic accessibility of this motif from biologically abundant 2-hydroxyacids.[19,30] We selected iron porphyrins as the metal scaffold for evaluation of radical binding and α-elimination. Iron has demonstrated metalation reactivity with alkyl radicals and has a rich history of carbene reactivity.[28,31–39] Further, iron can readily facilitate α-elimination when in the appropriate oxidation state, and such states can be controlled with photocatalysts.[28,29] Cyclopropanation was selected as a model reaction to capture evidence of putative carbene intermediates. This choice was motivated, in part, by the established reactivity of iron-mediated carbene insertion across olefins. Further motivation for using cyclopropanation was derived from the value of the resulting cyclopropane products to the industrial and academic communities.[40–43] In evaluating our proposed reaction sequence, we were excited to observe successful cyclopropanation of 2-(prop-1-en-2-yl)naphthalene by acetate-protected lactic acid (activated as an *N*-hydroxyphthalimide [NHPI] ester), using diethyl 1,4-dihydro-2,6-dimethyl-3,5-pyridinedicarboxylate **(**Hantzsch ester) as a sacrificial reductant, with catalytic 5,10,15,20-tetrakis(4-methoxyphenyl)-21H,23H-porphine iron(III) chloride (Fe(TMPP)Cl) and $Ir(dFCF_3ppy)_2dttbpyPF_6$ under blue light irradiation. This initial reaction provided critical proof-of-concept that a radical approach to carbene intermediates was a viable strategy; upon optimization, the desired cyclopropanated product was obtained in 95% yield (see SI for further details). Control experiments revealed the necessity of all reaction components; no product was formed in the absence of the iron catalyst, light, or Hantzsch ester. Diminished efficiency (36%) was observed in the absence of the iridium

photocatalyst, consistent with a Hantzsch ester-mediated electron donor-acceptor complex for radical generation (see extended data Fig. 1 for proposed catalytic cycle and Fig. S1 for further discussion).[44] Taken together, these initial experiments support the viability of our novel metallaphotoredox-mediated carbene generation and capture paradigm.

Having established the viability of this process for cyclopropanation, and with initial optimal conditions in hand, we sought to probe the scope of leaving groups viable for iron carbene formation. We synthesized NHPI esters of lactic acid derivatives possessing a range of non-traditional α-oxygenated leaving groups: α-phenoxy, α-methoxy, and α-hydroxy. Pleasingly, under the optimized conditions identified for the α-acetoxy system, all of these substrates were effective in the cyclopropanation (77–95% yield) (see Fig. S5). This tolerance led us to question whether leaving groups beyond oxygen-based systems would be viable. We investigated α-amino acids as precursors for iron carbenes using our net reductive reaction conditions. Using a range of amine protecting groups, we systematically evaluated the α-elimination step. Although most protecting groups were ineffective, including those within the expected nucleofugality range (see Fig. S8 for full list),[45–47] we observed that tosyl- and trifyl-protected α-amino acids furnished the desired cyclopropanated products in good yields. The extension to tosyl- and trifyl-amine leaving groups is a rare example of nitrogen-based leaving groups participating in substitution/elimination-type reactivity and an underexplored strategy for deaminative functionalization.[48–50] Reaction development resulted in the identification of six distinct leaving groups capable of serving as carbene precursors, demonstrating the tolerance of iron porphyrin α-elimination to a wide range of leaving group abilities (a range of over 10 pK_a units) and offering a modular strategy to access carbene intermediates (Fig. 1b).

Scope of cyclopropanation using iron carbene intermediates

With optimized cyclopropanation conditions in hand, we explored the scope of carboxylic acids and alkenes. We were excited to find both benzyl and alkyl carbenes, generated from α-acetoxy carboxylic acids, to be effective partners (Fig. 2). Styrenes (**1**) and electron-rich alkenes (**2**–**4**) smoothly underwent cyclopropanation, consistent with the well-established electrophilic reactivity of our proposed iron porphyrin carbene intermediate.[33] Benzyl carbamate (CBz)-protected dehydroalanine was cyclopropanated in moderate yield (**5**), revealing a mild and facile approach to peptide backbone modification. Importantly, complex scaffolds bearing a range of functional groups were found to undergo efficient metallaphotoredox cyclopropanation, demonstrating the amenability of this method to late-state functionalization (**6**–**8**). Tertiary amines, traditionally problematic under photoredox conditions due to competitive oxidation,[51,52] were well tolerated under a modified protocol involving addition of one equivalent of triflic acid to protonate the amine (**7**). An exploration of the scope of α-methoxy and α-phenoxy carboxylic acids again demonstrated that a range of substituted carbenes and alkenes perform well under the reaction conditions, including those containing medicinally relevant heteroaromatic rings (**9**–**15**).[53] Several amino acids underwent carbene formation, albeit with diminished reactivity and yields; tosyl-protected alanine, methionine sulfoxide, leucine, and lysine served as viable carbene precursors (**16**–**19**). We were excited to find that a diverse array of cyclopropanated scaffolds could be accessed using multiple variations of both the radical precursor and olefin coupling partners (see Fig. S14 for additional examples).

Beyond carboxylic acids as carbene precursors

Given that binding of a radical to a metal center is disconnected from the origin of that radical, we wondered whether this paradigm could be extended to alternate radical precursors beyond those derived from carboxylic acids. Early studies supported the generality of this approach; α-bromo acetates that are either commercially available or easily generated from the corresponding aldehydes can be engaged via silyl radical-mediated halogen atom abstraction (XAT).[54,55] Upon metalation of this alkyl radical species, controlled α-elimination generates the carbene intermediate, which in turn readily undergoes cyclopropanation (**20**–**26**) (Fig. 2, bottom).[19] This finding encouraged us to explore other precursors of carbenes that would be arduous or even dangerous to make by other means. We turned our attention to accessing fluoroalkyl carbenes en route to high value fluoroalkyl cyclopropanes. Fluoromethylated cyclopropanes have emerged as valuable motifs in pharmaceuticals, due to their metabolic stability and beneficial effect on pharmacokinetic and pharmacodynamic profiles.[56,57] Despite growing interest in these small carbocycles, fluoromethylated cyclopropanes are particularly challenging to access as they must currently be synthesized through diazo species, which pose substantial safety concerns.[58,59] Recently, *N*-hydroxyphthalimide activated β-fluoro alcohols have been shown to fragment to generate ketyl intermediates through a formal 1,2-hydrogen atom transfer (HAT) process (see Fig. S9 for proposed mechanism).[60,61] Owing to the presence of the hydroxy motif geminal to a C(sp^3)-radical, we hypothesized that these alcohol-derived ketyl

intermediates could serve as effective precursors to deliver fluoro-alkylated cyclopropane products through the metallaphotoredox carbene protocol described here. Using a readily accessible 2,2,2-trifluoroethylated NHPI ether, cyclopropanation proceeds smoothly when using styryl derivatives, including those with unprotected indoles (**29**) and carboxylic acids (**30**) (Fig. 3), demonstrating tolerance for acidic functionality that would be problematic using traditional carbene precursors due to their ylide-type character. Free amines are tolerated (**31**) under the acidic protonation strategy described earlier. Electron-deficient styrenes containing α-ester functionality undergo cyclopropanation in reasonable yield (**32**), and dienes are successfully converted to allylic trifluoromethylated cyclopropanes (**33**). An enamide derived from uracil exclusively reacts at the more electron-rich olefin (**34**), consistent with electrophilic iron porphyrin carbene reactivity.[33] Anilines and Cbz-protected amines are well-tolerated in the reaction, providing amino cyclopropane products (**35**–**37**). Less synthetically accessible cyclopropanes, such as a hydroxycyclopropane equivalent, can also be accessed via vinyl benzoate (**38**). Pharmaceutical compounds and complex drug-like scaffolds are cyclopropanated in high yields, demonstrating the high functional group tolerance of the method and the potential for application to late-stage functionalization (**39**–**46**). The use of 2,2-difluoroethanol as the starting material proved similarly effective, furnishing difluoromethyl-substituted cyclopropanes in moderate yields (**47**–**51**). By exploiting the ketyl-type fragmentation of β-fluoro NHPI-activated alcohols under reductive conditions, we obtained elusive di- and tri-fluoromethylated cyclopropanes under our mild reaction conditions.

σ-Bond insertion reactions

Beyond cyclopropanation, iron carbenes are known to undergo σ-bond insertion reactions due to their Fischer-type carbene character.[62] This reactivity provides another potential avenue to harness the transient carbenes generated via metallaphotoredox, while concurrently verifying the intermediacy of iron carbenes in this platform. Our efforts to achieve σ-bond insertion using our newly developed carbene platform proved successful. We were excited to observe successful insertion of β-fluoro alcohol and carboxylic acid-based systems into P–H bonds (Fig. 4, **52** and **53**). Extending this reactivity to thiophenol starting materials enabled the synthesis of (difluoro)alkylated thioether products (**54** and **55**). Furthermore, N–H alkylation of both anilines and amines proceeded smoothly, including on scaffolds containing medicinally important electron-deficient heteroarenes (**56**–**59**).[53] Monoalkylated amine products were obtained by reaction with NHPI-activated α-phenoxy propanoic acid, bypassing the conventional reactivity of amide bond formation (**60**). The successful demonstration of σ-bond insertion in these diverse settings further reveals the ability of carbene intermediates to engage in useful bond formations beyond annulation and establishes their power as reactive intermediates that may be effectively harnessed through our radical approach.

Outlook

In summary, we have disclosed a conceptually new platform that effectively accesses high-energy carbenes via the merger of iron catalysis with photoredox catalysis. Bench-stable and ubiquitous starting materials, such as carboxylic acids, amino acids, and alcohols, are readily converted to iron carbene intermediates through the energy of visible light. This approach overcomes the inherent limitations associated with accessing carbene reactivity using conventional methods and unlocks their potential as reactive intermediates under metallaphotoredox conditions from bench-stable starting materials using six types of underexplored leaving groups in reduction α-elimination steps. The utility of this method is exemplified by the variety of scaffolds that can be accessed via cyclopropanation and σ-bond insertion. The process described herein shows the broad tolerance for complexity that is characteristic of photochemical reactions. We anticipate this approach will appeal to academic and industrial practitioners alike as a new mechanistic approach to carbene generation and a powerful synthetic tool for exploiting carbene reactivity to enhance molecular complexity.

REFERENCES

1. Gessner, V. H. Stability and reactivity control of carbenoids: recent advances and perspectives. *Chem. Commun.* **52**, 12011–12023 (2016).
2. De Frémont, P., Marion, N. & Nolan, S. P. Carbenes: Synthesis, properties, and organometallic chemistry. *Coord. Chem. Rev.* **253**, 862–892 (2009).
3. Green, S. P. et al. Thermal stability and explosive hazard assessment of diazo compounds and diazo transfer reagents. *Org. Process Res. Dev.* **24**, 67–84 (2020).

4. Vaitla, J., Bayer, A. & Hopmann, K. H. Synthesis of indoles and pyrroles utilizing iridium carbenes generated from sulfoxonium ylides. *Angew. Chem. Int. Ed.* **56**, 4277–4281 (2017).
5. Müller, P., Fernandez, D., Nury, P. & Rossier, J.-C. Metal-catalyzed carbenoid reactions with iodonium and sulfonium ylides. *J. Phys. Org. Chem.* **11**, 321–333 (1998).
6. Gandelman, M., Rybtchinski, B., Ashkenazi, N., Gauvin, R. M. & Milstein, D. A new general method for the preparation of metal carbene complexes. *J. Am. Chem. Soc.* **123**, 5372–5373 (2001).
7. Slavík, P., Trowse, B. R., O'Brien, P. & Smith, D. K. Organogel delivery vehicles for the stabilization of organolithium reagents. *Nat. Chem.* **15**, 319–325 (2023).
8. Chan, A. Y. et al. Metallaphotoredox: The merger of photoredox and transition metal catalysis. *Chem. Rev.* **122**, 1485–1542 (2022).
9. Webb, E. W. et al. Nucleophilic (Radio)Fluorination of redox-active esters via radical-polar crossover enabled by photoredox catalysis. *J. Am. Chem. Soc.* **142**, 9493–9500 (2020).
10. Porter, N. J., Danelius, E., Gonen, T. & Arnold, F. H. Biocatalytic carbene transfer using diazirines. *J. Am. Chem. Soc.* **144**, 8892–8896 (2022).
11. Cannalire, R. et al. Visible light photocatalysis in the late-stage functionalization of pharmaceutically relevant compounds. *Chem. Soc. Rev.* **50**, 766–897 (2021).
12. Romero, N. A. & Nicewicz, D. A. Organic photoredox catalysis. *Chem. Rev.* **116**, 10075–10166 (2016).
13. Shaw, M. H., Twilton, J. & MacMillan, D. W. C. Photoredox catalysis in organic chemistry. *J. Org. Chem.* **81**, 6898–6926 (2016).
14. Horn, E. J., Rosen, B. R. & Baran, P. S. Synthetic organic electrochemistry: An enabling and innately sustainable method. *ACS Cent. Sci.* **2**, 302–308 (2016).
15. Empel, C. & Koenigs, R. M. Sustainable carbene transfer reactions with iron and light. *Synlett* **30**, 1929–1934 (2019).
16. Charette, A. B. & Beauchemin, A. Simmons-Smith cyclopropanation reaction. in *Organic Reactions* 1–415 (John Wiley & Sons, Ltd, 2004).
17. Afonso, C. A. M., Motherwell, W. B., O'Shea, D. M. & Roberts, L. R. An improved method for the generation of organozinc carbenoids and its application in dicarbonyl coupling reactions. *Tetrahedron Lett.* **33**, 3899–3902 (1992).
18. Ishikawa, S., Sheppard, T. D., D'Oyley, J. M., Kamimura, A. & Motherwell, W. B. A rapid route to aminocyclopropanes via carbamatoorganozinc carbenoids. *Angew. Chem. Int. Ed.* **52**, 10060–10063 (2013).
19. Zhang, L., DeMuynck, B. M., Paneque, A. N., Rutherford, J. E. & Nagib, D. A. Carbene reactivity from alkyl and aryl aldehydes. *Science* **377**, 649–654 (2022).
20. Zhang, L. & Nagib, D. A. Carbonyl cross-metathesis via deoxygenative gem-di-metal catalysis. *Nat. Chem.* **16**, 107-113 (2024).
21. DeMuynck, B. M., Zhang, L., Ralph, E. K. & Nagib, D. A. Cyclopropanation of unactivated alkenes with non-stabilized iron carbenes. *Chem* **10**, 1015–1027 (2024).
22. Jia, M. & Ma, S. New approaches to the synthesis of metal carbenes. *Angew. Chem. Int. Ed.* **55**, 9134–9166 (2016).
23. Wei, Y., Tinoco, A., Steck, V., Fasan, R. & Zhang, Y. Cyclopropanations via Heme carbenes: Basic mechanism and effects of carbene substituent, protein axial ligand, and porphyrin substitution. *J. Am. Chem. Soc.* **140**, 1649–1662 (2018).
24. Halpern, J. Determination of transition metal-alkyl bond dissociation energies from kinetic measurements. *Polyhedron* **7**, 1483–1490 (1988).
25. Johnson, M. W., Hannoun, K. I., Tan, Y., Fu, G. C. & Peters, J. C. A mechanistic investigation of the photoinduced, copper-mediated cross-coupling of an aryl thiol with an aryl halide. *Chem. Sci.* **7**, 4091–4100 (2016).
26. Goswami, M., Bruin, B. de & Dzik, W. I. Difluorocarbene transfer from a cobalt complex to an electron-deficient alkene. *Chem. Commun.* **53**, 4382–4385 (2017).
27. Neta, P. Radiation chemical studies of porphyrins and metalloporphyrins. in *Studies in Physical and Theoretical Chemistry* vol. 87 453–479 (Elsevier, 2001).
28. Guldi, D. M., Kumar, M., Neta, P. & Hambright, P. Reactions of alkyl and fluoroalkyl radicals with nickel, iron, and manganese porphyrins. *J. Phys. Chem.* **96**, 9576–9581 (1992).
29. Brault, D. & Neta, P. Reactions of iron porphyrins with trifluoromethyl, trifluoromethylperoxy, and tribromomethylperoxy radicals. *J. Phys. Chem.* **91**, 4156–4160 (1987).

30. Karmakar, S., Silamkoti, A., Meanwell, N. A., Mathur, A. & Gupta, A. K. Utilization of C(sp^3)-carboxylic acids and their redox-active esters in decarboxylative carbon−carbon bond formation. *Adv. Synth. Catal.* **363**, 3693–3736 (2021).
31. Liu, W., Lavagnino, M. N., Gould, C. A., Alcázar, J. & MacMillan, D. W. C. A biomimetic S_H2 cross-coupling mechanism for quaternary sp^3-carbon formation. *Science* **374**, 1258–1263 (2021).
32. Maldotti, A. et al. Photochemistry of iron-porphyrin complexes. Biomimetics and catalysis. *Coord. Chem. Rev.* **125**, 143–154 (1993).
33. Batista, V. F., G. A. Pinto, D. C. & Silva, A. M. S. Iron: A worthy contender in metal carbene chemistry. *ACS Catal.* **10**, 10096–10116 (2020).
34. Carreras, V., Tanbouza, N. & Ollevier, T. The power of iron catalysis in diazo chemistry. *Synthesis* **53**, 79–94 (2021).
35. Damiano, C., Sonzini, P. & Gallo, E. Iron catalysts with N-ligands for carbene transfer of diazo reagents. *Chem. Soc. Rev.* **49**, 4867–4905 (2020).
36. Lee, W.-C. C., Wang, D.-S., Zhu, Y. & Zhang, X. P. Iron(III)-based metalloradical catalysis for asymmetric cyclopropanation via a stepwise radical mechanism. *Nat. Chem.* **15**, 1569–1580 (2023).
37. Tanbouza, N., Keipour, H. & Ollevier, T. Fe II-catalysed insertion reaction of α-diazocarbonyls into X–H bonds (X = Si, S, N, and O) in dimethyl carbonate as a suitable solvent alternative. *RSC Adv.* **9**, 31241–31246 (2019).
38. Ma, C. et al. Synthesis and characterization of donor–acceptor iron porphyrin carbenes and their reactivities in N–H insertion and related three-component reaction. *J. Am. Chem. Soc.* **145**, 4934–4939 (2023).
39. Morandi, B. & Carreira, E. M. Iron-catalyzed cyclopropanation in 6 M KOH with *in situ* generation of diazomethane. *Science* **335**, 1471–1474 (2012).
40. Reissig, H.-U. & Zimmer, R. Donor−acceptor-substituted cyclopropane derivatives and their application in organic synthesis. *Chem. Rev.* **103**, 1151–1196 (2003).
41. Wu, W., Lin, Z. & Jiang, H. Recent advances in the synthesis of cyclopropanes. *Org. Biomol. Chem.* **16**, 7315–7329 (2018).
42. Chen, D. Y.-K., Pouwer, R. H. & Richard, J.-A. Recent advances in the total synthesis of cyclopropane-containing natural products. *Chem. Soc. Rev.* **41**, 4631–4642 (2012).
43. Gagnon, A., Duplessis, M. & Fader, L. Arylcyclopropanes: Properties, synthesis and use in medicinal chemistry. *Org. Prep. Proced. Int.* **42**, 1–69 (2010).
44. Yedase, G. S., Venugopal, S., P., A. & Yatham, V. R. Catalyst-free Hantzsch Ester-mediated organic transformations driven by visible light. *Asian J. Org. Chem.* **11**, e202200478 (2022).
45. Broeckaert, L., Moens, J., Roos, G., Proft, F. D. & Geerlings, P. Intrinsic nucleofugality scale within the framework of density functional reactivity theory. *J. Phys. Chem. A* **112**, 12164–12171 (2008).
46. Spahlinger, G. & Jackson, J. E. Nucleofugality in oxygen and nitrogen derived pseudohalides in Menshutkin reactions: the importance of the intrinsic barrier. *Phys. Chem. Chem. Phys.* **16**, 24559–24569 (2014).
47. Stirling, C. J. M. Leaving groups and nucleofugality in elimination and other organic reactions. *Acc. Chem. Res.* **12**, 198–203 (1979).
48. Berger, K. J. & Levin, M. D. Reframing primary alkyl amines as aliphatic building blocks. *Org. Biomol. Chem.* **19**, 11–36 (2021).
49. Katritzky, A. R. & Musumarra, G. New insights into aliphatic nucleophilic substitution reactions from the use of pyridines as leaving groups. *Chem. Soc. Rev.* **13**, 47 (1984).
50. Correia, J. T. M. et al. Photoinduced deaminative strategies: Katritzky salts as alkyl radical precursors. *Chem. Commun.* **56**, 503–514 (2020).
51. McNally, A., Prier, C. K. & MacMillan, D. W. C. Discovery of an α-amino C–H arylation reaction using the strategy of accelerated serendipity. *Science* **334**, 4 (2011).
52. Hu, J., Wang, J., Nguyen, T. H. & Zheng, N. The chemistry of amine radical cations produced by visible light photoredox catalysis. *Beilstein J. Org. Chem.* **9**, 1977–2001 (2013).
53. Rotella, D. P. Heterocycles in drug discovery: Properties and preparation. in *Advances in Heterocyclic Chemistry* vol. 134 149–183 (Elsevier, 2021).
54. Wang, L., Lear, J. M., Rafferty, S. M., Fosu, S. C. & Nagib, D. A. Ketyl radical reactivity via atom transfer catalysis. *Science* **362**, 225–229 (2018).
55. Huang, H.-M., Bellotti, P., Erchinger, J. E., Paulisch, T. O. & Glorius, F. Radical carbonyl umpolung arylation via dual nickel catalysis. *J. Am. Chem. Soc.* **144**, 1899–1909 (2022).

56. Grygorenko, O. O., Artamonov, O. S., Komarov, I. V. & Mykhailiuk, P. K. Trifluoromethyl-substituted cyclopropanes. *Tetrahedron* **67**, 803–823 (2011).
57. Wu, W.-F., Lin, J.-H., Xiao, J.-C., Cao, Y.-C. & Ma, Y. Recent advances in the synthesis of CF_3- or HCF_2-substituted cyclopropanes. *Asian J. Org. Chem.* **10**, 485–495 (2021).
58. Deadman, B. J., Collins, S. G. & Maguire, A. R. Taming hazardous chemistry in flow: The continuous processing of diazo and diazonium compounds. *Chem. – Eur. J.* **21**, 2298–2308 (2015).
59. Mykhailiuk, P. K. 2,2,2-Trifluorodiazoethane (CF_3CHN_2): A long journey since 1943. *Chem. Rev.* **120**, 12718–12755 (2020).
60. Zhang, J. et al. Visible-light-induced alkoxyl radicals enable α-C(sp^3)-H bond allylation. *iScience* **23**, 100755 (2020).
61. Lombardi, L. et al. Direct synthesis of α-aryl-α-trifluoromethyl alcohols via nickel catalyzed cross-electrophile coupling. *Angew. Chem. Int. Ed.* **61**, e202211732 (2022).
62. Dötz, K. H. & Stendel, J. Fischer carbene complexes in organic synthesis: Metal-assisted and metal-templated reactions. *Chem. Rev.* **109**, 3227–3274 (2009).

Fig 1 | Enabling carbene reactivity via radical intermediates a. Radical starting materials as alternatives to hazardous and limiting traditional carbene precursors. **b.** General approach to iron carbene reactivity through carboxylic acids, amino acids, and alcohol precursors using metallaphotoredox for cyclopropanation and σ-bond insertion. Me, methyl; Boc, *tert*-butyloxycarbonyl; Et, ethyl; Bz, benzoyl; Nphth, phthalimide; Ac, acetyl; Tf, trifluoromethylsulfonyl; Ts, 4-toluenesulfonyl; Ph, phenyl. LG corresponds to α-elimination leaving group and varies based on radical precursor utilized.

Fig 2 | Scope of photoredox-enabled iron carbene cyclopropanation using carboxylic acids as precursors. α-Acetoxy, α-methoxy, α-phenoxy carboxylic acids, α-amino acids, and α-bromo acetates can be used as carbene precursors. Experiments run with 1.0 equiv. of olefin, 2.0 equiv. carbene precursor, 3.0 equiv. Hantzsch ester or 3.5 equiv. $AdNHSi(TMS)_3$, 7.5 mol% iron catalyst, and 2 mol% Ir photocatalyst irradiating using a Penn Integrated Photoreactor with 450 nm plates for 12 hours. For amine containing substrates, 1.0 equiv. trifluoromethanesulfonic acid (TfOH) was added to the reaction prior to irradiation. Isolated yields shown except where noted. Major diastereomer shown (d.r. reported from crude reaction mixtures and is relative stereochemistry around cyclopropane). *^{1}H NMR yield using 1,3,5-trimethoxybenzene as an internal standard. See Supplementary Information for experimental details. LG, leaving group; HE, Hantzsch ester; Si•, $AdNHSi(TMS)_3$; Boc, *tert*-butyloxycarbonyl; Bn, benzyl; Et, ethyl; Ph, phenyl; Me, methyl; Cbz, benzyl oxycarbonyl; NPhth, phthalimide; Ts, 4-toluenesulfonyl; Ac, acetyl; tBu, *tert*-butyl, iPr, isopropyl.

Fig 3 | Scope of tri- and difluoromethyl cyclopropanation through carbene metallaphotoredox. Formal 1,2-HAT ketyl radical generation for carbene reactivity from β-fluoro alcohols. Experiments run with 1.0 equiv. of olefin, 2.0 equiv. carbene precursor, 3.0 equiv. Hantzsch ester, 7.5 mol% iron catalyst, and 2 mol% Ir photocatalyst irradiating using a Penn Integrated Photoreactor with 450 nm plates for 12 hours. For amine containing substrates, 1.0 equiv. trifluoromethanesulfonic acid (TfOH) was added to the reaction prior to irradiation. Isolated yields shown except where noted. Major diastereomer shown (d.r. reported from crude reaction mixtures and is relative stereochemistry around cyclopropane). See Supplementary Information for experimental details. *^{19}F NMR yield using 4-fluoro methylbenzoate as an internal standard. Boc, *tert*-butyloxycarbonyl; Bn, benzyl; Et, ethyl; Ph, phenyl; Me, methyl; Cbz, benzyl oxycarbonyl; NPhth, phthalimide; Ac, acetyl; Bz, benzoyl; nProp, normal propyl; tBu; *tert*-butyl, iPr, isopropyl.

Fig. 4 | σ-bond insertions through metallaphotoredox carbene formation. P–H, S–H, and N–H insertion is viable using carboxylic acid and alcohol derived precursors through iron carbene intermediates. Experiments run with 1.0 equiv. of olefin, 2.0 equiv. carbene precursor, 3.0 equiv. Hantzsch ester, 7.5 mol% iron catalyst, and 2 mol% Ir photocatalyst irradiating using a Penn Integrated Photoreactor with 450 nm plates for 12 hours. Isolated yields shown. See Supplementary Information for experimental details. Ph, phenyl; Me, methyl; NPhth, phthalimide.

Methods

General procedure for cyclopropanation using α-oxy carboxylic acid precursors. An oven dried 4 mL (≤ 0.5 mmol scale) or 40 mL (> 0.5 mmol scale) vial equipped with a stir bar was charged with the $Ir(dFCF_3ppy)_2dttbpyPF_6$ (2 mol%), Fe(TMPP)Cl (7.5 mol%), Hantzsch ester (3 equiv), alkene/styrene (1.0 equiv), and redox active ester (2 equiv). *N*,*N*-dimethylacetamide (DMA) (0.1 M) was then added, and the vial sealed with a cap. The reaction solution was sparged with N_2 for 2 minutes followed by an 8 minute sparge of the vial headspace (as a precaution for volatile substrates). Following sparging, the vial was sealed with parafilm and placed in a Penn integrated photoreactor and irradiated for 12 hours at 450 nm (100% light intensity, max fans (5200 rpm), 500 rpm stir rate). After irradiation, the reaction was diluted with H_2O and Et_2O and the organic layer was extracted (Et_2O extraction typically performed 3x). The combined organic layers were then washed with brine, dried ($MgSO_4$ or $NaSO_4$), and filtered over celite. The filtrate was then concentrated under reduced vacuum

and the resulting residue was purified using flash column chromatography (SiO_2) to afford the cyclopropanated product.

General procedure for cyclopropanation using α-amino acid precursors. An oven dried 4 mL (≤ 0.5 mmol scale) or 40 mL vial (> 0.5 mmol scale) equipped with a stir bar was charged with the $Ir(ppy)_2dttbpyPF_6$ (2 mol%), Fe(TPP)Cl (5.0 mol%), tBuHantzsch ester (3.75 equiv), alkene/styrene (1.0 equiv), and redox active ester (2.5 equiv). Acetone (0.1 M) was then added, and the vial sealed with a cap. The reaction solution was sparged with N_2 for 2 minutes followed by an 8 minute sparge of the vial headspace (as a precaution for volatile substrates). Following sparging, the vial was sealed with parafilm and placed in a Penn integrated photoreactor and irradiated for 12 hours at 450 nm (10% light intensity, max fans (5200 rpm), 500 rpm stir rate). After irradiation, the reaction was diluted with H_2O and Et_2O and the organic layer was extracted (Et_2O extraction typically performed 3x). The combined organic layers were then washed with brine, dried ($MgSO_4$ or $NaSO_4$), and filtered over celite. The filtrate was then concentrated under reduced vacuum and the resulting residue was purified using flash column chromatography (SiO_2) to afford the cyclopropanated product.

General procedure for cyclopropanation using α-bromo acetate precursors. An oven dried 4 mL (≤ 0.5 mmol scale) or 40 mL (> 0.5 mmol scale) vial equipped with a stir bar was charged with the $Ir(ppy)_2dttbpyPF_6$ (1.5 mol%), Fe(OEP)Cl (5.0 mol%), adamantyl aminosilane (4.50 equiv), alkene/styrene (1.0 equiv), and bromoacetate (3.5 equiv). Dichloroethane (0.1 M) was then added, and the vial sealed with a cap. The reaction solution was sparged with N_2 for 2 minutes followed by an 8 minute sparge of the vial headspace (as a precaution for volatile substrates). Following sparging, the vial was sealed with parafilm and placed in a Penn integrated photoreactor and irradiated for 12 hours at 450 nm (100% light intensity, max fans (5200 rpm), 500 rpm stir rate). After irradiation, the reaction was diluted with H_2O and Et_2O and the organic layer was extracted (Et_2O extraction typically performed 3x). The combined organic layers were then washed with brine, dried ($MgSO_4$ or $NaSO_4$), and filtered over celite. The filtrate was then concentrated under reduced vacuum and the resulting residue was purified using flash column chromatography (SiO_2) to afford the cyclopropanated product.

General procedure for cyclopropanation using β-trifluoromethyl alcohol precursors. An oven dried 4 mL (≤ 0.5 mmol scale) or 40 mL (> 0.5 mmol scale) vial equipped with a stir bar was charged with the $Ir(dFCF_3ppy)_2dttbpyPF_6$ (2 mol%), Fe(TMPP)Cl (7.5 mol%), Hantzsch ester (3 equiv), alkene/styrene (1.0 equiv), and 2-(2,2,2-trifluoroethoxy)isoindoline-1,3-dione (2 equiv). DMA (0.1 M) was then added, and the vial sealed with a cap. The reaction solution was sparged with N_2 for 2 minutes followed by an 8 minute sparge of the vial headspace (as a precaution for volatile substrates). Following sparging, the vial was sealed with parafilm and placed in a Penn integrated photoreactor and irradiated for 12 hours at 450 nm (100% light intensity, max fans (5200 rpm), 500 rpm stirrate). After irradiation, the reaction was diluted with H_2O and Et_2O and the organic layer was extracted (Et_2O extraction typically performed 3x). The combined organic layers were then washed with brine, dried ($MgSO_4$ or $NaSO_4$), and filtered over celite. The filtrate was then concentrated under reduced vacuum and the resulting residue was purified using flash column chromatography (SiO_2) to afford the cyclopropanated product.

General procedure for cyclopropanation using β-difluoromethyl alcohol precursors. An oven dried 4 mL (≤ 0.5 mmol scale) or 40 mL vial (> 0.5 mmol scale) equipped with a stir bar was charged with the $Ir(dFCF_3ppy)_2dttbpyPF_6$ (2 mol%), Fe(TMPP)Cl (15 mol%), Hantzsch ester (3 equiv), alkene/styrene (1.0 equiv), and 2-(2,2,2-trifluoroethoxy)isoindoline-1,3-dione (2 equiv). DMA (0.1 M) was then added, and the vial sealed with a cap. The reaction solution was sparged with N_2 for 2 minutes followed by an 8 minute sparge of the vial headspace (as a precaution for volatile substrates). Following sparging, the vial was sealed with parafilm and placed in a Penn integrated photoreactor and irradiated for 12 hours at 450 nm (10% light intensity, max fans (5200 rpm), 500 rpm stir rate). After irradiation, the reaction was diluted with H_2O and Et_2O and the organic layer was extracted (Et_2O extraction typically performed 3x). The combined organic layers were then washed with brine, dried ($MgSO_4$ or $NaSO_4$), and filtered over celite. The filtrate was then concentrated under reduced vacuum and the resulting residue was purified using flash column chromatography (SiO_2) to afford the cyclopropanated product.

General procedure for X-H bond insertions. An oven dried 4 mL (≤ 0.5 mmol scale) or 40 mL (> 0.5 mmol scale) vial equipped with a stir bar was charged with the $Ir(dFCF_3ppy)_2dttbpyPF_6$ (2 mol%), Fe(TMPP)Cl (7.5

mol%), Hantzsch ester (3 equiv), nucleophile (1.0 equiv), and redox active ester (2 equiv). DMA (0.1 M) was then added, and the vial sealed with a cap. The reaction solution was sparged with N_2 for 2 minutes followed by an 8 minute sparge of the vial headspace (as a precaution for volatile substrates). Following sparging, the vial was sealed with parafilm and placed in a Penn integrated photoreactor and irradiated for 12 hours at 450 nm (100% light intensity, max fans (5200 rpm), 500 rpm stir rate). After irradiation, the reaction was diluted with H_2O and Et_2O and the organic layer was extracted (Et_2O extraction typically performed 3x). The combined organic layers were then washed with brine, dried ($MgSO_4$ or $NaSO_4$), and filtered over celite. The filtrate was then concentrated under reduced vacuum and the resulting residue was purified using flash column chromatography (SiO_2) to afford the σ-bond insertion product.

Acknowledgements: The authors acknowledge Amy Y. Chan, Prof. Ciaran P. Seath, Dr. James A. Rossi-Ashton, Dr. Russell T. Smith, Dr. Colin A. Gould, and Alice Long for chemical discussions. The authors also thank Rebecca M. Lambert for assistance with the preparation of this manuscript. Research reported in this work was supported by the National Institute of General Medical Sciences (NIGMS) of the National Institutes of Health (R35GM134897), the Princeton Catalysis Initiative, Janssen R&D, and kind gifts from Merck, Pfizer, Bristol-Myers Squibb, Genentech, and Genmab. The content is solely the responsibility of the authors and does not necessarily represent the official views of NIGMS.

Author contributions: D.W.C.M., N.W.D., and B.T.B. conceptualized the radical approach to carbenes. B.T.B., N.W.D., C.B.K., and M.C.B. designed the experiments. B.T.B. and N.W.D. performed and analyzed the experiments. B.T.B., C.B.K., M.C.B., N.W.D., and D.W.C.M. prepared the manuscript. D.W.C.M. directed the project. *These authors contributed equally to this work: Benjamin T. Boyle and Nathan W. Dow.

Competing interests:
D. W. C. M. declares an ownership interest in Penn PhD photoreactor, which is used to irradiate reactions in this work. The other authors declare no competing interests.

Supporting Information

All supporting information is linked to the online version of the paper at www.nature.com/nature.

Data availability

All data supporting the findings of this study are available in the main text or in the supplementary information.

Author information

Reprints and permissions information is available at www.nature.com/reprints. Readers are welcome to comment on the online version of the paper. Correspondence and requests for materials should be addressed to D.W.C.M. (dmacmill@princeton.edu)

Corresponding Author

David W. C. MacMillan – *Merck Center for Catalysis at Princeton University, Princeton, New Jersey 08544, United States*
Email: dmacmill@princeton.edu

Extended Data Fig. 1 | Proposed mechanism for iron porphyrin carbene formation through metallaphotoredox catalysis. Metallaphotoredox-mediated formation of iron porphyrin carbene intermediates exploiting a single-electron reduction mediated α-elimination. Me, methyl; Et, ethyl, Ac, acetyl; Phth, phthalimide; $HEH^{\bullet+}$, oxidized Hantzsch ester; Ir, $Ir(dFCF_3ppy)_2dttbpy$; Fe, iron porphyrin. For further commentary and discussion see Fig. S1.

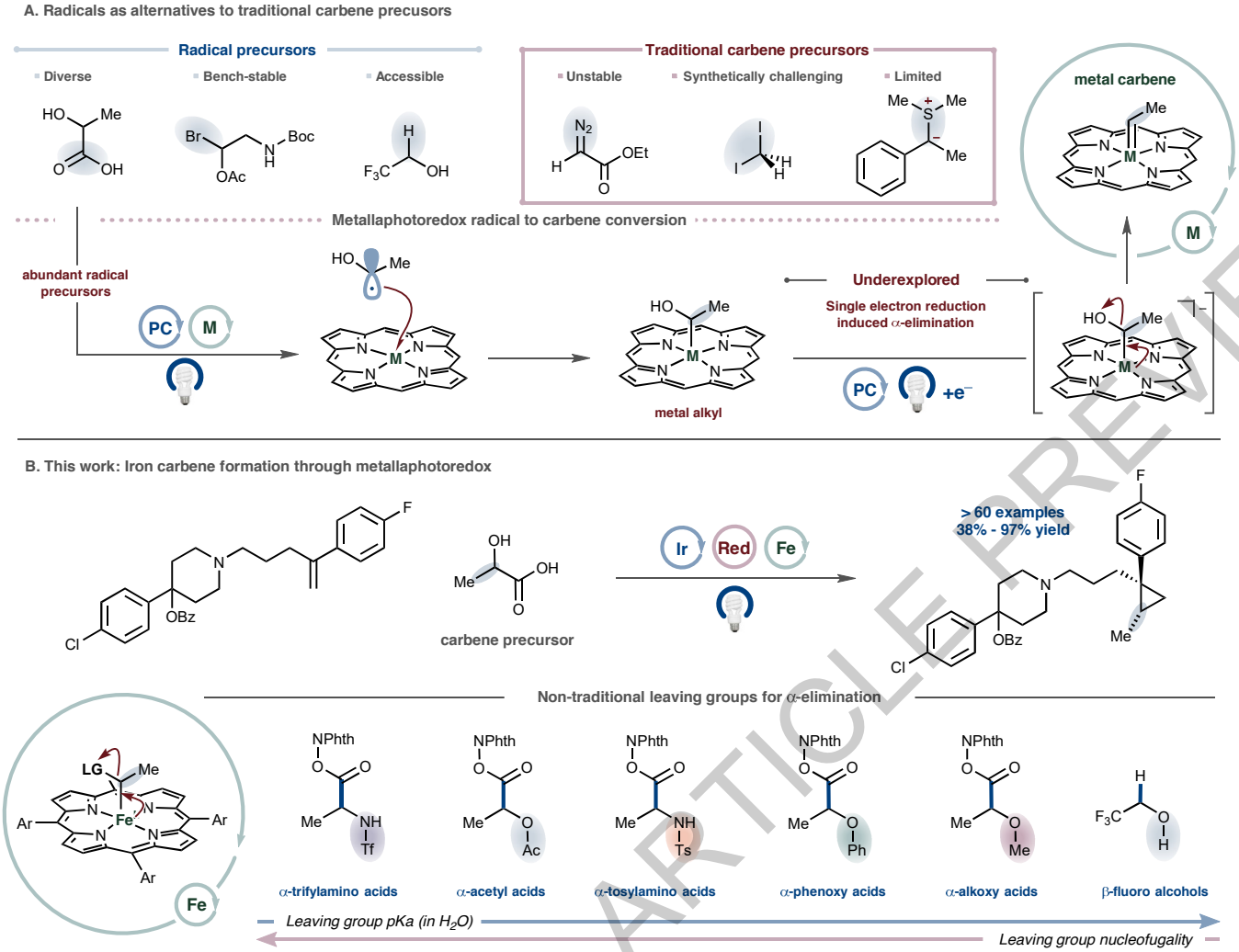

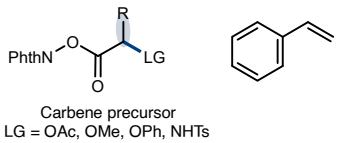

Carbene precursor
LG = OAc, OMe, OPh, NHTs

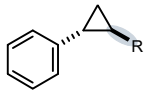

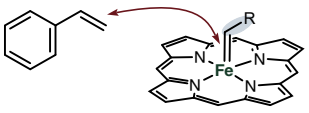

Iron Carbene cyclopropanation

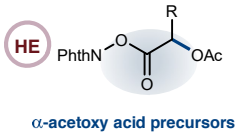

α-acetoxy acid precursors

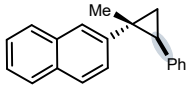

1, 55% >20:1 d.r.

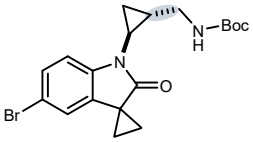

2, 58% 6.9:1 d.r.

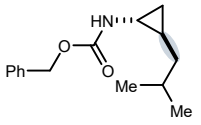

3, 59% 4:1 d.r.

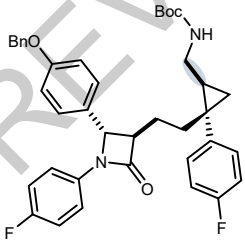

from O-Bn Ezetimibe
8, 74% 1.1:1 d.r.

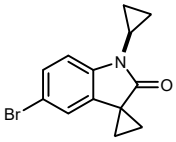

4, 73%

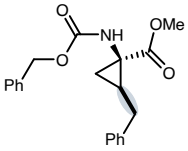

from N-Cbz dehydroalanine
5, 54% 1.5:1 d.r.

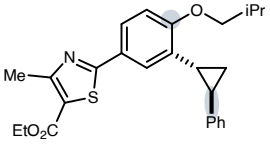

from Febuxostat
6, 56% 1.5:1 d.r.

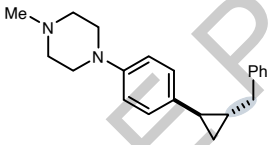

7, 72% 10:1 d.r.

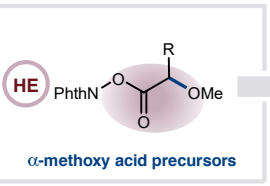

α-methoxy acid precursors

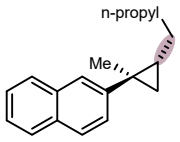

9, 65% 1.5:1 d.r.

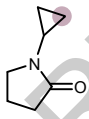

10, 95%

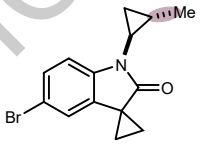

11, 63% 5:1 d.r.

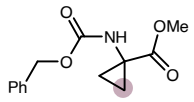

from N-Cbz dehydroalanine
12, 87%

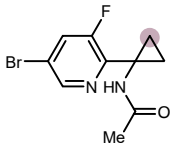

13, 68%

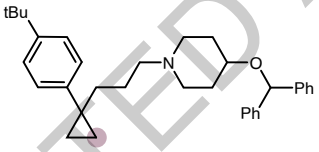

from Ebastine
14, 70%

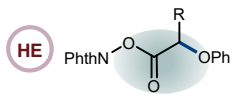

α-phenoxy acid precursors

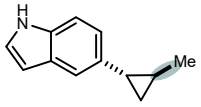

15, 65% 4.8:1 d.r.

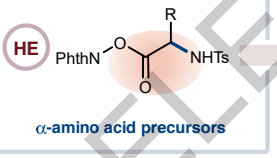

α-amino acid precursors

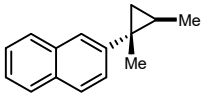

from alanine
16, 63% 1.6:1 d.r.

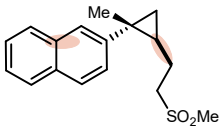

from methionine sulfoxide
17, 43% 3:1 d.r.

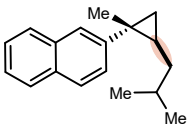

from leucine
18, 47% 1.6:1 d.r.

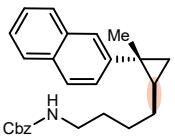

from N-Cbz lysine
19, 41% 1.9:1 d.r.

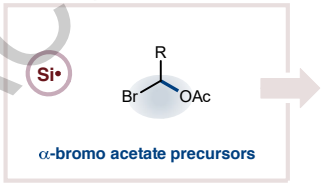

α-bromo acetate precursors

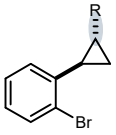

20, R = H: 60%
21, R = Me: 61% 8.3:1 d.r.

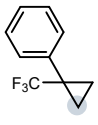

22, 63%

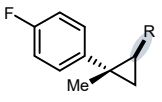

23, R = H: 82%
24, R = Me: 97% 7.7:1 d.r.

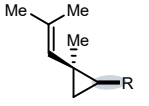

25, R = H: 91%*
26, R = Me: 85%* 1.4:1 d.r.

α-CF_3 or α-CF_2H carbene precursor
1 step from corresponding fluoroethanol

X = F or H
CF_2X-cyclopropane

Trifluoromethyl cyclopropane

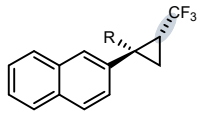

27, R = Me: 87% >20:1 d.r.
28, R = H: 75% >20:1 d.r.

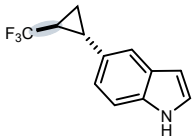

29, 92% >20:1 d.r.

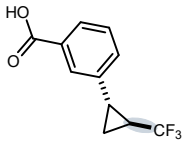

30, 77% >20:1 d.r.

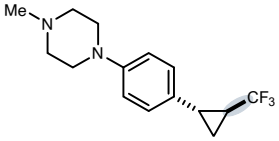

31, 74% >20:1 d.r.

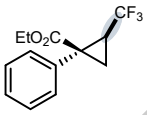

32, 58% 3.6:1 d.r.

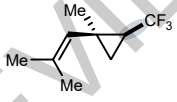

33, 59%* 1.3:1 d.r.

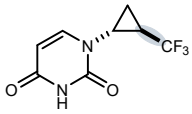

34, 49% >20:1 d.r.

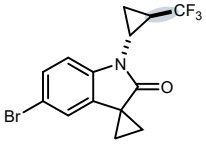

35, 65% >20:1 d.r.

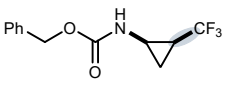

36, 95% 2.2:1 d.r.

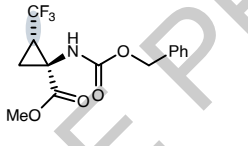

from N-CBz dehydroalanine
37, 54% 1.5:1 d.r.

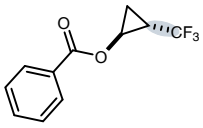

38, 42% 4:1 d.r.

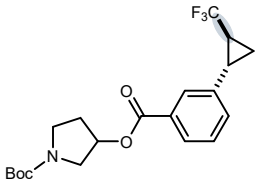

39, 70% >20:1 d.r.

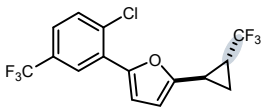

40, 60% 3:1 d.r.

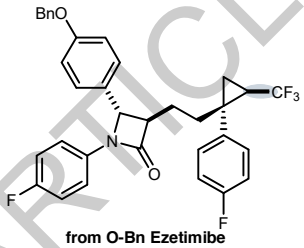

from O-Bn Ezetimibe
41, 77% 2.5:1 d.r.

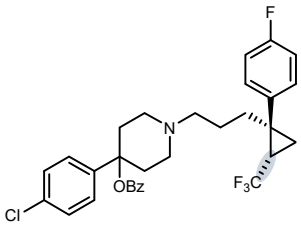

from O-Bz haloperidol
42, 74% >20:1 d.r.

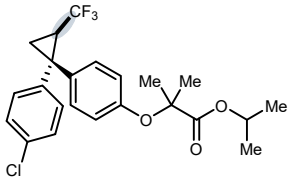

from Fenofibrate
43, 65% 1.3:1 d.r.

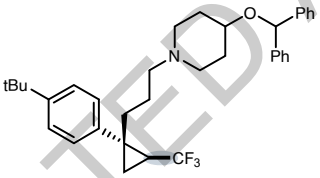

from Ebastine
44, 81% 2.9:1 d.r.

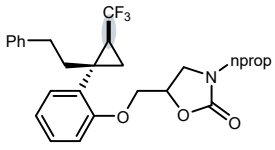

from Propafenone
45, 47% 4.5:1 d.r.

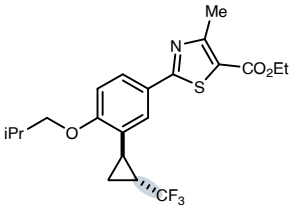

from Febuxostat
46, 50% >20:1 d.r.

Difluoromethyl cyclopropane

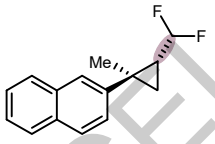

47, 63% 13.5:1 d.r.

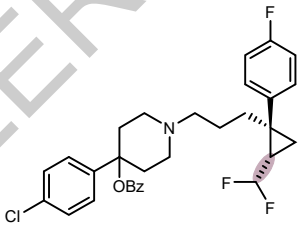

from O-Bz haloperidol
48, 55% 6.9:1 d.r.

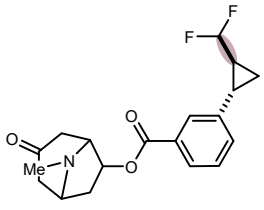

49, 48% >20:1 d.r.

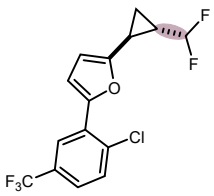

50, 41% >20:1 d.r.

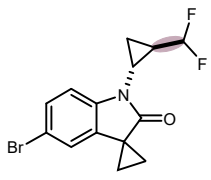

51, 45% 5:1 d.r.

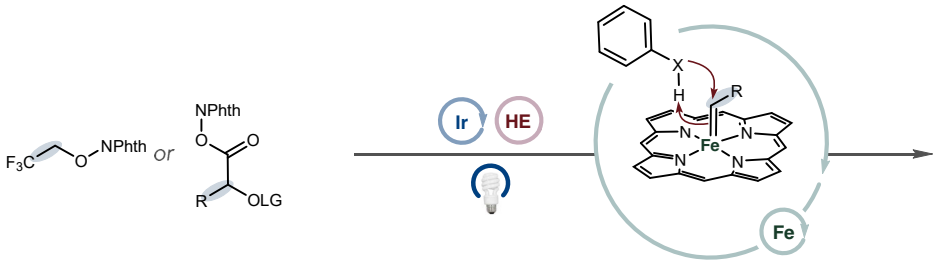

P-H insertion

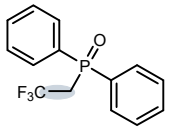

52, 60%

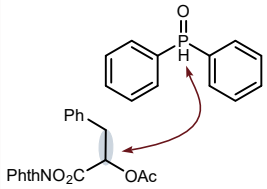

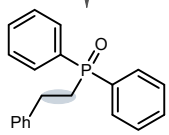

53, 55%

S-H insertion

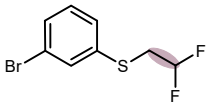

54, 43%

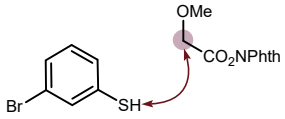

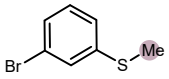

55, 56%

N-H insertion

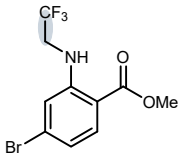

56, 67%

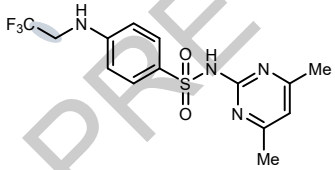

from sulfamethazine
57, 54%

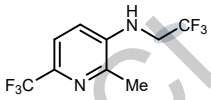

58, 63%

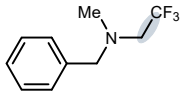

59, 38%

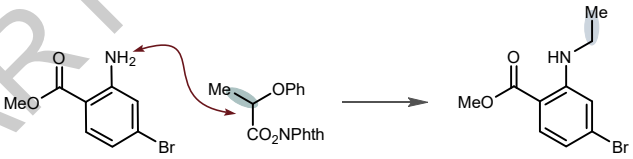

60, 64%

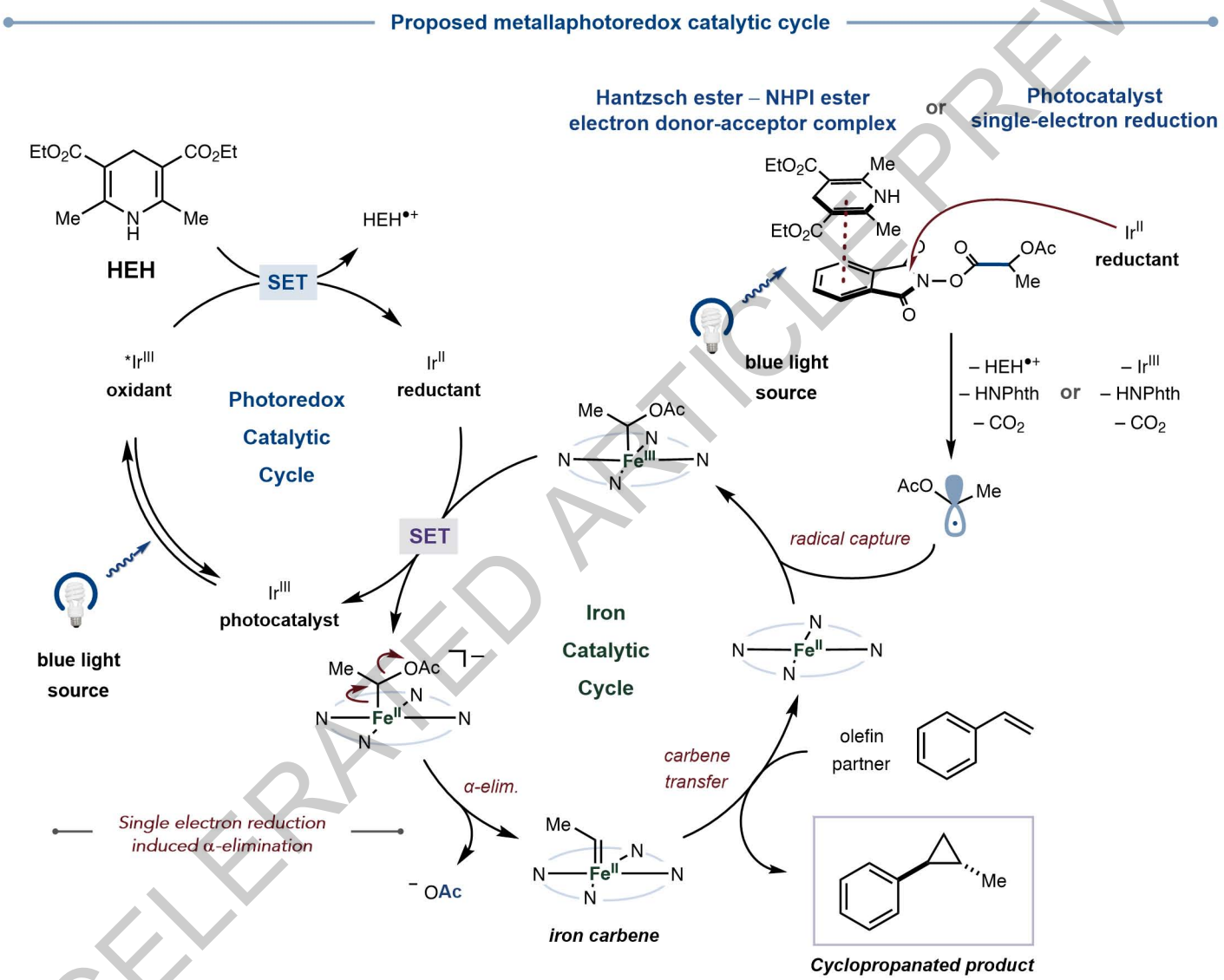

Extended Data Fig. 1